Chapter 2

The Method of Moments

In this book, we are concerned with solving surface integral equations. Because closed-form analytic solutions are unavailable for most problems, in practice we must apply numerical methods. In this chapter we will introduce the Method of Moments (MoM), a technique that is used to convert integral equations into a linear system that can then be solved numerically by computer. To begin, we will analyze a few simple electrostatic problems to provide a bit of context, and then formally define the MoM. We will next discuss the expansion of an unknown function by a sum of weighted basis functions, and compare and contrast point matching and the Method of Galerkin. In the chapters that follow, we will then discuss electrodynamic problems and numerical methods for solving a general system of linear equations. Having covered this material, we will then be ready to apply the MoM to the more challenging integral equation problems in later chapters.

2.1 Electrostatic Problems

Because electrostatic problems are relatively simple compared to the electrodynamic case, they provide a good context for introducing algorithms used to solve integral equations. Recall that the electric potential ϕ_e at a point $\mathbf{r}$ due to an electric charge density q_e is given by the integral

$$\phi_e(\mathbf{r}) = \int_V \frac{q_e(\mathbf{r}')}{4\pi\epsilon|\mathbf{r}-\mathbf{r}'|}\, d\mathbf{r}'. \tag{2.1}$$

If we know $q_e(\mathbf{r}')$, we can obtain the electric potential everywhere. If we instead know the electric potential $\phi_e(\mathbf{r})$ but not the charge density, (2.1) becomes an integral equation for $q_e(\mathbf{r}')$. We will now solve this problem numerically for a pair of practical examples, a charged wire and plate.

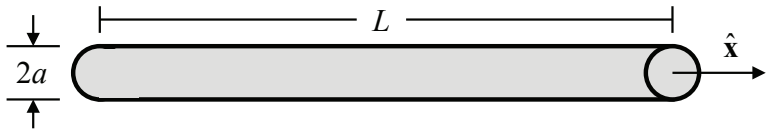


Figure 2.1: Thin Wire Dimensions

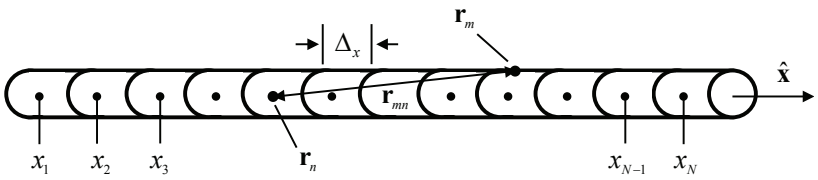


Figure 2.2: Thin Wire Segmentation

2.1.1 Charged Wire

Consider a thin, conducting wire of length L and radius a oriented along the x axis, as shown in Figure 2.1. If the radius of the wire is very small compared to the length ($a \ll L$), the electric potential on the wire can be expressed via the integral

$$\phi_e(\mathbf{r}) = \int_0^L \frac{q_e(x')}{4\pi\epsilon|\mathbf{r}-\mathbf{r}'|}\, dx' \,, \tag{2.2}$$

where $q_e(x')$ is the line-charge density, and

$$|\mathbf{r}-\mathbf{r}'| = \sqrt{(x-x')^2+(y-y')^2}\,. \tag{2.3}$$

We intend to convert (2.2) into a linear system of equations, so we first subdivide the wire into N subsegments, each having length Δ_x, as shown in Figure 2.2. Within each subsegment, we assume that the charge density has a constant value such that $q_e(x')$ is piecewise constant over the length of the wire. Mathematically, this can be written as

$$q_e(x') = \sum_{n=1}^{N} a_n f_n(x') \,, \tag{2.4}$$

where a_n are unknown coefficients, and $f_n(x')$ is a pulse function having a constant value on segment n but zero on all others, i.e.

$$f_n(x') = \begin{cases} 0 & x' < (n-1)\Delta_x \\ 1 & (n-1)\Delta_x \le x' \le n\Delta_x \\ 0 & x' > n\Delta_x \end{cases}. \tag{2.5}$$

We now set the potential of the wire to $\phi_e = 1$ V. Substituting (2.4) into (2.2) then yields

$$1 = \int_0^L \sum_{n=1}^{N} a_n f_n(x') \frac{1}{4\pi\epsilon|\mathbf{r}-\mathbf{r}'|}\, dx'. \tag{2.6}$$

Using the previous definition of the pulse function, we can rewrite this as

$$1 = \frac{1}{4\pi\epsilon} \sum_{n=1}^{N} a_n \int_{(n-1)\Delta_x}^{n\Delta_x} \frac{1}{|\mathbf{r} - \mathbf{r}'|}\, dx' \,, \tag{2.7}$$

where we now have a sum of integrals, each over the domain of a single pulse function. Let us now fix the source points so that they are on the wire axis, and the field points to be on the wire's surface. This ensures that we do not encounter a singularity in the integrand. The denominator of the integrand now becomes

$$|\mathbf{r} - \mathbf{r}'| = \sqrt{(x - x')^2 + a^2} \tag{2.8}$$

and (2.7) can be written as

$$\begin{aligned} 4\pi\epsilon = a_1 \int_0^{\Delta_x} \frac{1}{\sqrt{(x-x')^2 + a^2}}\, dx' + a_2 \int_{\Delta_x}^{2\Delta_x} \frac{1}{\sqrt{(x-x')^2 + a^2}}\, dx' + \cdots \\ + a_{N-1} \int_{(N-2)\Delta_x}^{(N-1)\Delta_x} \frac{1}{\sqrt{(x-x')^2 + a^2}}\, dx' + a_N \int_{(N-1)\Delta_x}^{N\Delta_x} \frac{1}{\sqrt{(x-x')^2 + a^2}}\, dx' \,, \end{aligned} \tag{2.9}$$

which comprises a single equation in N unknowns. If we can now convert this into N equations in N unknowns, we can solve it by common matrix algebra routines. To do so, let us choose N independent field points x_m on the surface of the wire, each at the center of a wire segment. Doing so yields

$$\begin{aligned} 4\pi\epsilon &= a_1 \int_0^{\Delta_x} \frac{1}{\sqrt{(x_1-x')^2 + a^2}}\, dx' + \cdots + a_N \int_{(N-1)\Delta_x}^{N\Delta_x} \frac{1}{\sqrt{(x_1-x')^2 + a^2}}\, dx' \\ &\vdots \\ 4\pi\epsilon &= a_1 \int_0^{\Delta_x} \frac{1}{\sqrt{(x_N-x')^2 + a^2}}\, dx' + \cdots + a_N \int_{(N-1)\Delta_x}^{N\Delta_x} \frac{1}{\sqrt{(x_N-x')^2 + a^2}}\, dx' \,, \end{aligned} \tag{2.10}$$

which comprises a matrix system of the form

$$\begin{bmatrix} Z_{11} & Z_{12} & Z_{13} & \dots & Z_{1N} \\ Z_{21} & Z_{22} & Z_{23} & \dots & Z_{2N} \\ Z_{31} & Z_{32} & Z_{33} & \dots & Z_{3N} \\ \vdots & \vdots & \vdots & \ddots & \vdots \\ Z_{N1} & Z_{N2} & Z_{N3} & \dots & Z_{NN} \end{bmatrix} \begin{bmatrix} a_1 \\ a_2 \\ a_3 \\ \vdots \\ a_N \end{bmatrix} = \begin{bmatrix} b_1 \\ b_2 \\ b_3 \\ \vdots \\ b_N \end{bmatrix} \,, \tag{2.11}$$

where the matrix elements Z_{mn} are

$$Z_{mn} = \int_{(n-1)\Delta_x}^{n\Delta_x} \frac{1}{\sqrt{(x_m - x')^2 + a^2}}\, dx' \,, \tag{2.12}$$

and the right-hand side (RHS) vector elements b_m are

$$b_m = 4\pi\epsilon \,. \tag{2.13}$$

2.1.1.1 Matrix Element Evaluation

The integral in (2.12) can be evaluated in closed form. Performing this integration yields [1] (200.01)

$$Z_{mn} = \log\left[\frac{(x_b - x_m) + \sqrt{(x_b - x_m)^2 + a^2}}{(x_a - x_m) + \sqrt{(x_a - x_m)^2 + a^2}}\right], \tag{2.14}$$

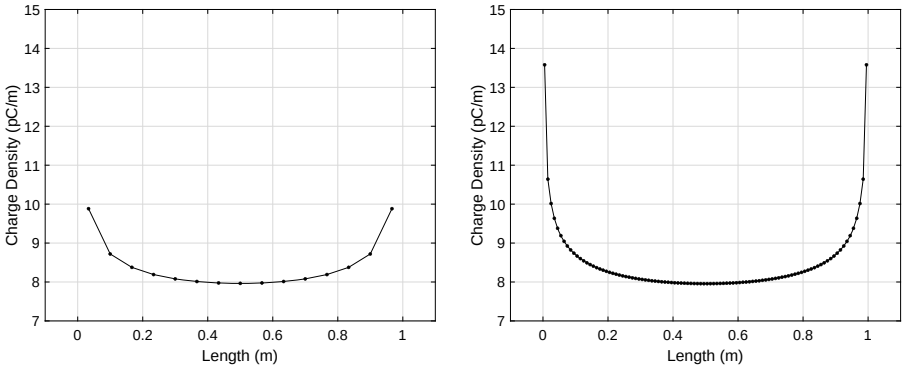
where $x_b = n\Delta_x$ and $x_a = (n-1)\Delta_x$. Note that the linear geometry of this problem yields a matrix that has a symmetric Toeplitz structure of the form

$$\mathbf{Z} = \begin{bmatrix} Z_1 & Z_2 & Z_3 & \dots & Z_N \\ Z_2 & Z_1 & Z_2 & \dots & Z_{N-1} \\ Z_3 & Z_2 & Z_1 & \dots & Z_{N-2} \\ \vdots & \vdots & \vdots & \ddots & \vdots \\ Z_N & Z_{N-1} & Z_{N-2} & \dots & Z_1 \end{bmatrix}, \tag{2.15}$$

where the elements from just the first row can be used to populate the entire matrix. Note, however, that a Toeplitz structure is not typically found in MoM matrices.

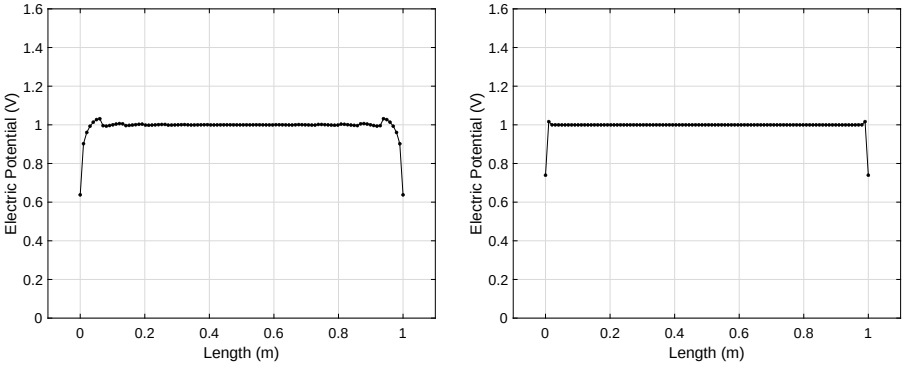
2.1.1.2 Solution

In Figures 2.3a and 2.3b is plotted the computed charge density on the wire using 15 and 100 segments, respectively. The density at the lower discretization level is somewhat crude, as expected. Increasing the discretization to 100 unknowns greatly improves the fidelity of the result. Using this charge density, we then compute the potential at 100 points along the wire using (2.2) and (2.14). The potential using 15 charge segments is shown in Figure 2.4a. While the potential is near the expected value of 1V, it is not of constant value, particularly near the ends of the wire. Figure 2.4b shows the potential obtained using 100 segments. The potential is now nearly constant across the entire wire, except at the endpoints. As a uniform segment size was used, the charge density tends to be oversampled in the middle of the wire and undersampled near the ends. As a result, the variation of the charge near the ends of the wire is not epresented as accurately as in the center, and the computed potential diverges from the true value. Realistic objects often have irregular surface features such as cracks, gaps, and corners that give rise to a more rapid variation in the solution at those points. To increase accuracy, it is advantageous to employ a denser level of discretization in areas where the most variation is expected.



(a) 15 Segments (b) 100 Segments

Figure 2.3: Straight Wire Charge Distribution



(a) 15 Segments (b) 100 Segments

Figure 2.4: Straight Wire Potential

2.1.2 Charged Plate

We next consider a similar problem involving a thin, charged conducting square plate of side length L, as shown in Figure 2.5. The potential on the plate can be written as

$$\phi_e(\mathbf{r}) = \int_{-\frac{L}{2}}^{\frac{L}{2}} \int_{-\frac{L}{2}}^{\frac{L}{2}} \frac{q_e(x', y')}{4\pi\epsilon|\mathbf{r} - \mathbf{r}'|}\, dx'\, dy' \,, \tag{2.16}$$

where $q_e(x', y')$ is now a surface charge density. Setting the plate to a potential of 1 V as before, (2.16) can be written as

$$4\pi\epsilon = \int_{-\frac{L}{2}}^{\frac{L}{2}} \int_{-\frac{L}{2}}^{\frac{L}{2}} \frac{q_e(x', y')}{\sqrt{(x - x')^2 + (y - y')^2}}\, dx'\, dy' \,. \tag{2.17}$$

We now subdivide the plate into N square patches, each having an edge length of $2a$ and area $\Delta_s = 4a^2$, and we assume that the charge is constant within each patch.

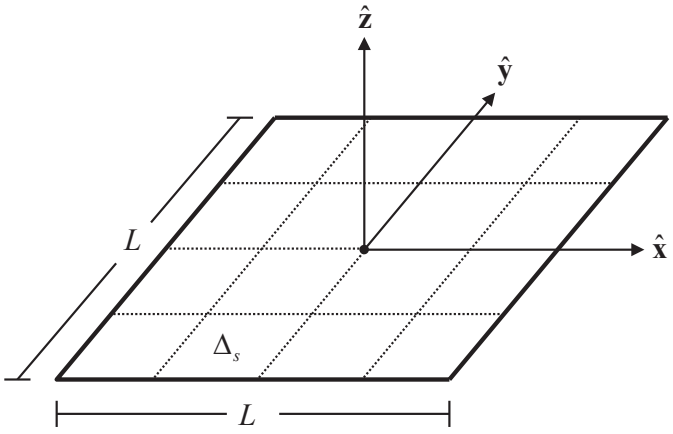


Figure 2.5: Thin Charged Plate Dimensions

We choose N independent field points, each located at the center (x_m, y_m) of a patch. Doing so yields a matrix equation with elements Z_{mn} given by

$$Z_{mn} = \int_{S_n} \frac{1}{\sqrt{(x_m - x')^2 + (y_m - y')^2}}\, dx'\, dy' \,, \tag{2.18}$$

where S_n comprises the extents of patch n. The elements in the right-hand side vector are the same as in (2.13).

2.1.2.1 Matrix Element Evaluation

When the source and field patches are the same ($m = n$), the integrand in (2.18) has an integrable singularity and must be evaluated analytically. These matrix elements are called *self terms*, and represent the most dominant interactions between elements. We will devote significant attention to the evaluation of self-term matrix elements in this book. The self-term integral for the charged plate is

$$Z_{mm} = \int_{-a}^{a}\int_{-a}^{a} \frac{1}{\sqrt{(x')^2 + (y')^2}}\, dx'\, dy' \,. \tag{2.19}$$

Performing the innermost integration yields [1] (200.01)

$$Z_{mm} = \int_{-a}^{a} \log\Big[\frac{\sqrt{a^2 + (y')^2} + a}{\sqrt{a^2 + (y')^2} - a}\Big] dy' \tag{2.20}$$

and performing the outermost integration then yields [2]

$$Z_{mm} = 2a \log\Big[y + \sqrt{a^2 + y^2}\Big] + y \log\left[\frac{y^2 + 2a\big(a + \sqrt{a^2 + y^2}\big)}{y^2}\right]\Bigg|_{-a}^{a} \,. \tag{2.21}$$

To evaluate (2.21), we make the substitution $s = \sqrt{a^2 + y^2}$, and noting that $y^2 = s^2 - a^2$, the numerator in the second logarithm can be written as

$$y^2 + 2a\big(a + \sqrt{a^2 + y^2}\big) = y^2 + 2a(a + s) = s^2 + a^2 + 2as = (s + a)^2 \ , \quad (2.22)$$

and (2.21) now becomes

$$Z_{mm} = 2a \log \Big[y + s \Big] + 2y \log \left[\frac{s + a}{|y|} \right] \Bigg|_{-a}^{a} . \quad (2.23)$$

Performing the substitution then yields

$$Z_{mm} = 2a \log \left[\frac{(1 + \sqrt{2})}{(\sqrt{2} - 1)} \right] + 4a \log(1 + \sqrt{2}) \ , \quad (2.24)$$

and noting that

$$\sqrt{2} - 1 = \frac{1}{\sqrt{2} + 1} \ , \quad (2.25)$$

the self term in (2.19) finally reduces to

$$Z_{mm} = 8a \log(1 + \sqrt{2}) \ . \quad (2.26)$$

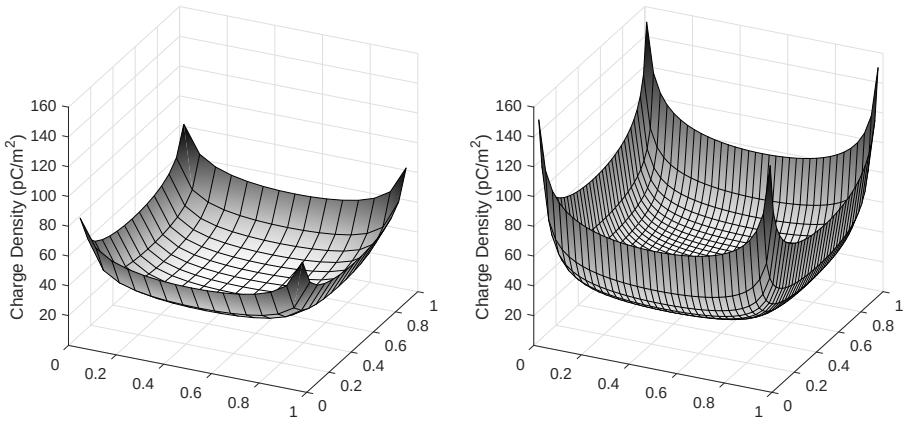
For patches that do not overlap ($m \neq n$) we will use a simple centroidal approximation to the integral, resulting in

$$Z_{mn} = \frac{\Delta_s}{\sqrt{(x_m - x_n)^2 + (y_m - y_n)^2}} \ , \quad (2.27)$$

where x_n and y_n are at the center of the source patch. Though this approximation is not very accurate for elements that are close to one another, it illustrates how to solve the problem. For a more accurate solution, analytic or adaptive numerical integration should be used instead. Matrix elements involving source and field points that do not overlap but are still sufficiently close are called *near terms*, and will also be considered in greater detail in this book.

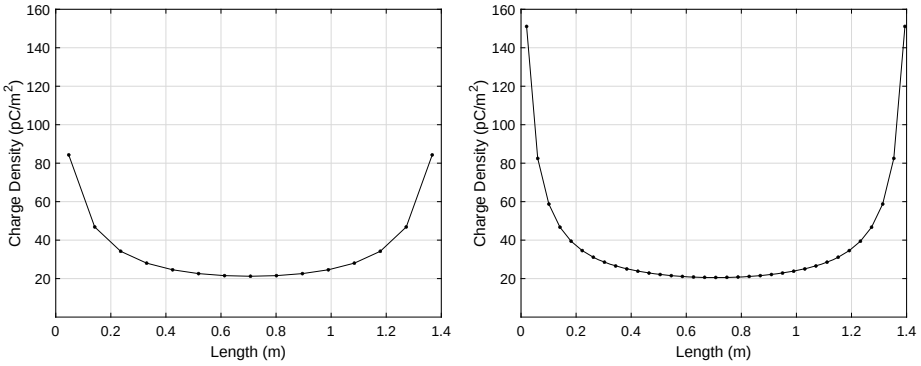
2.1.2.2 Solution

Figures 2.6a and 2.6b show the computed surface charge density obtained using 15 and 35 patches in the x and y directions, which comprises 225 and 1225 unknowns, respectively. Figures 2.7a and 2.7b show the surface charge density on the patches along the diagonal of the plate. As with the thin wire, the charge accumulates near the corners and the edges of the plate, and our solution would likely benefit from additional discretization density in those areas.



(a) 225 Patches (b) 1225 Patches

Figure 2.6: Charge Distribution on Square Plate



(a) 225 Patches (b) 1225 Patches

Figure 2.7: Potential on Square Plate Diagonal

2.1.2.2.1 Alternate Self-Term Integral Evaluation

Many surface integrals can be challenging to solve, and often a change in basis or coordinate system may help to make the solution more tractable. To illustrate, consider again the self-term in (2.19). As the integrand is even in x and y, we can restrict the integration to just the first quadrant as

$$Z_{mm} = 4 \int_0^a \int_0^a \frac{1}{\sqrt{(x')^2 + (y')^2}} \, dx' \, dy' \, . \tag{2.28}$$

Let us now move to polar coordinates, where

$$x = r \cos\theta \, , \quad y = r \sin\theta \, , \tag{2.29}$$

and

$$\frac{1}{\sqrt{(x')^2+(y')^2}} = \frac{1}{r}\,, \quad dx'\,dy' = \frac{1}{r} r dr d\theta\,. \tag{2.30}$$

Noting that

$$r = x\sec\theta \quad 0 \le \theta \le \pi/4 \tag{2.31}$$

and

$$r = y\csc\theta \quad \pi/4 \le \theta \le \pi/2\,, \tag{2.32}$$

allows us to then write

$$Z_{mm} = 4\int_0^{\pi/4}\int_0^{a\sec\theta} dr d\theta + 4\int_{\pi/4}^{\pi/2}\int_0^{a\csc\theta} dr d\theta\,, \tag{2.33}$$

and then,

$$Z_{mm} = 4a\int_0^{\pi/4}\sec\theta d\theta + 4a\int_{\pi/4}^{\pi/2}\csc\theta d\theta\,. \tag{2.34}$$

Following (4.3.116) and (4.3.117) in [3], both integrals evaluate to

$$\int_{\pi/4}^{\pi/2}\csc\theta d\theta = \log(\csc\theta - \cot\theta)\Big|_{\pi/4}^{\pi/2} = \log(1+\sqrt{2}) \tag{2.35}$$

and

$$\int_0^{\pi/4}\sec\theta d\theta = \log(\sec\theta + \tan\theta)\Big|_0^{\pi/4} = \log(1+\sqrt{2})\,, \tag{2.36}$$

and so,

$$Z_{mm} = 8a\log(1+\sqrt{2})\,. \tag{2.37}$$

2.2 The Method of Moments

In the previous section, we considered the problem of computing an unknown charge distribution on a thin wire or plate at a known potential. Our basic approach was to expand the unknown quantity using a set of known functions with unknown coefficients. We then converted the resulting equation into a linear system of equations by enforcing the boundary conditions, in this case the electric potential, at a number of field points on the object. The resulting linear system was then solved numerically for the unknown coefficients. Let us formalize this process by introducing a method of weighted residuals known as the Method of Moments. Consider the generalized problem

$$L(f) = g \tag{2.38}$$

where L is a linear operator, g is a known forcing function, and f is unknown [4]. In electromagnetic problems, L is typically an integro-differential operator such as $\mathcal{L}$ (3.77) and $\mathcal{K}$ (3.78), f is the unknown function (current) and g is a known driving function (incident field). Let us now expand f into a sum of N weighted basis functions

$$f = \sum_{n=1}^{N} a_n f_n \tag{2.39}$$

where a_n are unknown coefficients. Because L is linear, substitution of the above into (2.38) yields

$$\sum_{n=1}^{N} a_n L(f_n) \approx g \tag{2.40}$$

where the residual is

$$R = g - \sum_{n=1}^{N} a_n L(f_n) \; . \tag{2.41}$$

The basis functions f_n are chosen so they model the expected behavior of the unknown function throughout its domain, and they may be scalars or vectors depending on the problem. If the basis functions have local support in the domain, they are called *local* or *subsectional* basis functions. If their support spans the entire problem domain, they are called *global* or *entire-domain* basis functions. In this book we focus almost exclusively on local basis functions.

Let us now generalize the method by which the boundary conditions were previously enforced. We define an inner product or *moment* between a basis function $f_n(\mathbf{r}')$ and a *testing* or *weighting* function $f_m(\mathbf{r})$

$$\langle f_m, f_n \rangle \; = \int_{f_m} f_m(\mathbf{r}) \cdot \int_{f_n} f_n(\mathbf{r}') \; d\mathbf{r}' d\mathbf{r} \tag{2.42}$$

where the integrals can be line, surface, or volume integrals depending on the support of the basis and testing functions. Requiring the inner product of each testing function with the residual function to be zero yields

$$\sum_{n=1}^{N} a_n \langle f_m, L(f_n) \rangle \; = \; \langle f_m, g \rangle \tag{2.43}$$

which results in the $N \times N$ matrix equation $\mathbf{Za} = \mathbf{b}$ with matrix elements

$$Z_{mn} \; = \; \langle f_m, L(f_n) \rangle \tag{2.44}$$

and right-hand side vector elements

$$b_m \; = \; \langle f_m, g \rangle \; . \tag{2.45}$$

In electromagnetic problems, basis functions interact with all others via the Green's function and the resulting system matrix is full. This can be compared to other algorithms such as the Finite Element Method, where the matrix is typically sparse, symmetric, and banded, and many elements of each matrix row are zero [5].

2.2.1 Point Matching

In Sections 2.1.1 and 2.1.2, we enforced the boundary conditions by testing the integral equation at a set of discrete points on the object. This is equivalent to using a delta function as the testing function in (2.42), resulting in

$$f_m(\mathbf{r}) = \delta(\mathbf{r} - \mathbf{r}_m) \; . \tag{2.46}$$

This method, referred to as *point matching* or *point collocation*, offers advantages as well as disadvantages. One benefit is that in evaluating the matrix elements, no integral is required over the range of the testing function, only that of the source function, which may make evaluation of the matrix elements easier. The primary disadvantage is that the boundary conditions are matched only at discrete locations throughout the solution domain. Regardless, the results are often still reasonable, and we will use this method for a few problems in this book for comparative purposes.

2.2.2 Galerkin's Method

For testing, we are free to use whatever functions we wish. However, for most problems, the choice of testing function is crucial to obtaining a good solution. One of the most commonly used is the *Method of Galerkin*, where the basis functions are used as the testing functions. Galerkin testing enforces the boundary condition in a weighted-residual sense over the solution domain, instead of at discrete points as with point matching. However, this comes at the expense of increased complexity and computation time required to evaluate the matrix elements. Most of the MoM problems encountered in the literature use Galerkin testing as the standard method (with its use often assumed or implied), and we will do so as well for most of the problems in this book.

2.3 Common One-Dimensional Basis Functions

The most important characteristic of a basis function is that it can reasonably represent the behavior of the unknown function throughout its domain. If the solution has a high level of variation in a particular region, pulse basis functions may not be as good a choice as a linear or higher-order function. The choice of basis function also determines the level of difficulty in evaluating the MoM matrix elements, which in some cases may be quite high. We will now briefly consider some one-dimensional local basis functions commonly used in Moment Method problems.

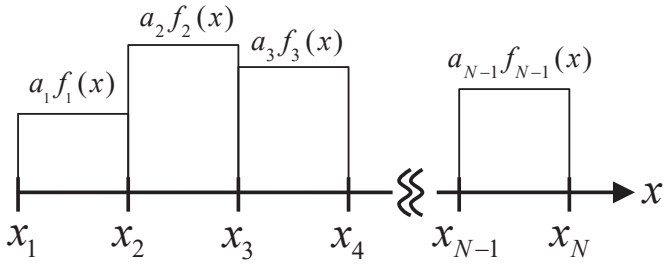


Figure 2.8: Pulse Functions

2.3.1 Pulse Functions

A set of pulse basis functions is depicted in Figure 2.8, where the domain has been divided into N points with $N-1$ subsegments/pulses. In our figure the segments all have equal lengths, however, this is not required. A pulse function is defined as

$$f_n(x) = 1 \qquad x_n \leq x \leq x_{n+1} \tag{2.47}$$

and zero otherwise. Pulse functions comprise a simple and rather crude approximation to the solution over each segment, but can greatly simplify the evaluation of MoM matrix elements. Note that since the derivative of pulse functions is impulsive, they cannot be used when the integral operator contains a derivative with respect to x [6].

2.3.2 Piecewise Triangular Functions

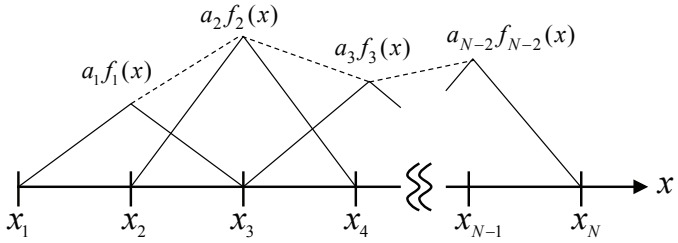


Figure 2.9: Triangle Functions (End Condition 1)

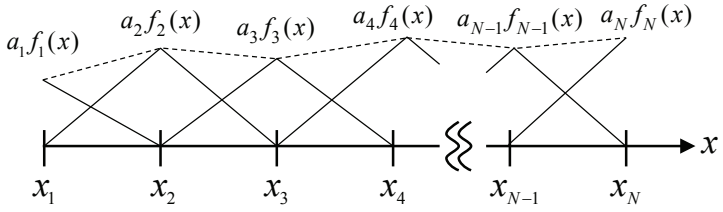


Figure 2.10: Triangle Functions (End Condition 2)

Where pulse functions are constant on a single segment, a triangle function spans two segments and varies from zero at the outer points to unity at the center. A set of triangle functions is shown in Figure 2.9. The domain has been divided into N points and $N-1$ subsegments, resulting in $N-2$ basis functions. Although we have again shown the segments as having equal length, this is not required. Since adjacent functions overlap by one segment, triangles provide a piecewise linear variation of the solution between segments. The triangle function is defined as

$$f_n(x) = \frac{x - x_{n-1}}{x_n - x_{n-1}} \qquad x_{n-1} \leq x \leq x_n \tag{2.48}$$

and

$$f_n(x) = \frac{x_{n+1} - x}{x_{n+1} - x_n} \qquad x_n \leq x \leq x_{n+1} \; . \tag{2.49}$$

Triangle functions can be used when the integral operator contains a derivative with respect to x, which is useful in redistributing vector derivatives.

Note that the configuration in Figure 2.9 forces the solution to zero at x_1 and x_N. This may be desirable when the value of the solution at the ends of the domain is known to be zero *a priori*, however it should not be used when the solution might be nonzero. In this case, we can assign a *half triangle* to the first and last segments, which allows the solution to take on any value at the ends. This is illustrated in Figure 2.10, where we now have a total of N basis functions.

2.3.3 Piecewise Sinusoidal Functions

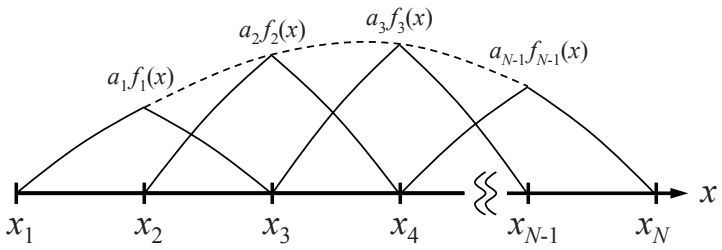


Figure 2.11: Piecewise Sinusoidal Functions

Piecewise sinusoid functions are similar to triangle functions, as illustrated in Figure 2.11. They are sometimes used in the analysis of wire antennas because of their ability to represent sinusoidal current distributions. These functions are defined as

$$f_n(x) = \frac{\sin k(x - x_{n-1})}{\sin k(x_n - x_{n-1})} \qquad x_{n-1} \leq x \leq x_n \tag{2.50}$$

and

$$f_n(x) = \frac{\sin k(x_{n+1} - x)}{\sin k(x_{n+1} - x_n)} \qquad x_n \leq x \leq x_{n+1} \tag{2.51}$$

where k is the wavenumber, and the length of the segments is generally much less than the period of the sinusoid.

2.3.4 Number of Basis Functions

For a given problem, the number of basis functions (and thus, unknowns) must be chosen so that local variations in the solution are accurately modeled. As in this book we are concerned with time-harmonic problems, we must model amplitude as well as phase behavior. For linear basis functions such as the triangle in Section 2.3.2, a common "rule of thumb" is that at least ten unknowns per wavelength are needed to represent a sinusoid. This number should be increased in areas where the solution may

vary significantly, such as gaps, cracks, and edges on a surface. Also note that in problems having multiple dielectric regions, the wavelength in each material will differ and so must the density of the basis functions on the different material interfaces. Higher-order basis functions also exist that can reduce the unknown count at the expense of increased complexity in describing the surface geometry, as well as the MoM formulation and evaluation of matrix elements. Functions such as these are covered in detail in advanced references on basis functions in electromagnetics.

Though the number of unknowns N always increases with the size of the problem, the rate of increase depends on whether the problem domain is a line, surface, or volume. Given M discretization intervals per dimension, N typically varies as $N \sim O(M^d)$, where d is the number of dimensions. Thus, N will vary as $O(N)$ for one-dimensional problems, such as the thin-wire problems in Chapter 5, and $O(N^2)$ for the surface problems in Chapter 8. The resulting number may be as small as a few hundred, or may grow into the thousands or even millions for very large problems. This has significant consequences in terms of system memory, as it requires the storage of an $N \times N$ matrix. It also significantly affects the matrix solution time, which for direct methods, such as LU decomposition, have a time complexity of $O(N^3)$. We will consider compressive methods for very large problems in later chapters, which help to alleviate both of these issues.

References

[1] H. B. Dwight, *Tables of Integrals and Other Mathematical Data*. The Macmillan Company, 1961.

[2] *The Integrator*. Wolfram Research, integrals.wolfram.com.

[3] M. Abramowitz and I. Stegun, *Handbook of Mathematical Functions*. National Bureau of Standards, 1966.

[4] R. F. Harrington, *Field Computation by Moment Methods*. The Macmillan Company, 1968.

[5] J. Jin, *The Finite Element Method in Electromagnetics*. John Wiley and Sons, 1993.

[6] N. Morita, N. Kumagai, and J. R. Mautz, *Integral Equation Methods for Electromagnetics*. Artech House, 1990.